

See discussions, stats, and author profiles for this publication at: <https://www.researchgate.net/publication/26247676>

Mesoporous Silica Nanoparticle-Based Double Drug Delivery System for Glucose-Responsive Controlled Release of Insulin and Cyclic AMP

ARTICLE in JOURNAL OF THE AMERICAN CHEMICAL SOCIETY · JULY 2009

Impact Factor: 12.11 · DOI: 10.1021/ja901831u · Source: PubMed

CITATIONS

383

READS

573

4 AUTHORS, INCLUDING:



Brian G Trewyn

Colorado School of Mines

63 PUBLICATIONS 6,923 CITATIONS

[SEE PROFILE](#)



Igor Ivan Slowing

U.S. Department of Energy, Ames Laboratory

53 PUBLICATIONS 5,641 CITATIONS

[SEE PROFILE](#)

Mesoporous Silica Nanoparticle-Based Double Drug Delivery System for Glucose-Responsive Controlled Release of Insulin and Cyclic AMP

Yannan Zhao, Brian G. Trewyn, Igor I. Slowing, and Victor S.-Y. Lin*

*Department of Chemistry, U.S. Department of Energy Ames Laboratory, Iowa State University,
Ames, Iowa 50011-3111*

Received March 9, 2009; E-mail: vsylin@iastate.edu

Stimuli-responsive controlled-release systems have attracted much attention for their potential applications in the area of drug and gene delivery.^{1–3} In particular, surface-functionalized, end-capped mesoporous silica nanoparticle (MSN) materials have been demonstrated as efficient stimuli-responsive controlled-release systems having the advantageous “zero premature release” property. The biocompatibility of MSN both in vitro and in vivo has been demonstrated by several recent studies.^{4–7} Furthermore, literature reports on the biodistribution and circulation properties of MSN administered in animals by intravenous injection have highlighted the promising potential of these multifunctional nanoparticles for in vivo biomedical applications and organ-specific delivery of therapeutics.

In contrast to nonporous nanoparticles, MSN offers both interior pore and exterior particle surfaces for loading different guest molecules. This is particularly useful for controlling the sequence of release for different cargos, which is crucial for the efficacy of many codelivery applications. These codelivery systems with control over the sequence of release could play a key role in overcoming several current challenges in therapy. For example, conventional glucose-responsive insulin delivery systems suffer from the decrease of insulin release with repeated cycles.^{8,9} This problem could be overcome if the secretion of insulin from live cells could also be induced by sequential delivery of cyclic adenosine monophosphate (cAMP), which activates Ca^{2+} channels of pancreas beta cells and hence stimulates insulin secretion.^{10,11} However, because of the poor membrane permeability of cAMP, many attempts have been made to develop cAMP analogues¹² with good membrane permeability to study the insulin secretion mechanism. Unfortunately, to the best of our knowledge, no report of intracellular cAMP delivery by any drug carriers to control insulin production has appeared in the literature.

Herein, we report on the synthesis of a glucose-responsive MSN-based double delivery system for both insulin and cAMP with precise control over the sequence of release. As depicted in Figure 1a, gluconic acid-modified insulin (G-Ins)⁸ proteins are immobilized on the exterior surface of MSN and also serve as caps to encapsulate cAMP molecules inside the mesopores of MSN. The release of both G-Ins and cAMP from MSN can be triggered by the introduction of saccharides, such as glucose. Also, we have demonstrated that the uncapped MSN can be efficiently endocytosed by live mammalian cells, leading to effective intracellular release of the cell-membrane-impermeable cAMP.

We first synthesized an aminopropyl-functionalized (1.6 mmol g^{-1}) mesoporous silica nanosphere material (AP-MSN) with an average particle diameter of 120 nm and an MCM-41-type channel-like mesoporous structure (BJH pore diameter = 2.3 nm) via a method that we previously reported.¹³ The particle size is small enough ($\leq 200 \text{ nm}$) to evade rapid sequestration by phagocytic cells of the spleen and to allow long blood circulation.¹⁴ As

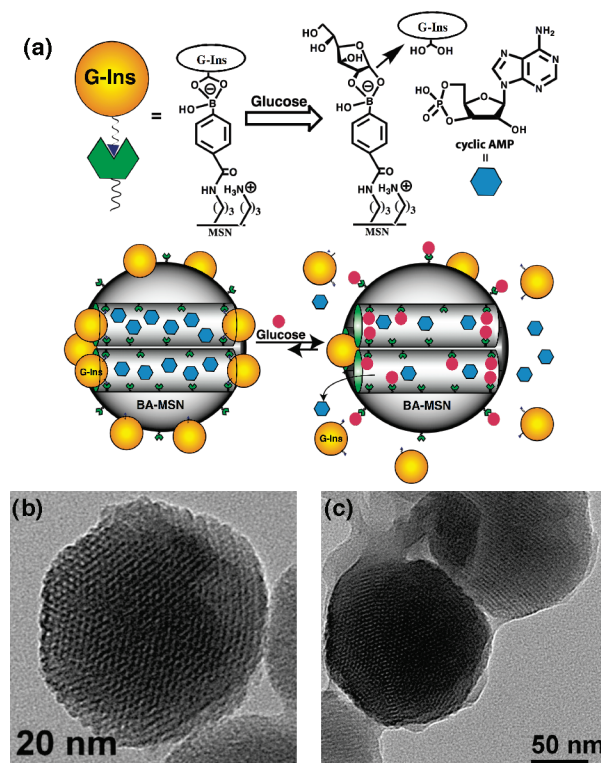


Figure 1. (a) Schematic representation of the glucose-responsive MSN-based delivery system for controlled release of bioactive G-Ins and cAMP. Transmission electron micrographs of (b) boronic acid-functionalized MSN and (c) FITC-G-Ins-capped MSN.

described in the Supporting Information (SI), 4-carboxyphenylboronic acid (0.15 g), *N*-hydroxysuccinimide (0.10 g), and 1-ethyl-3-(3-dimethylaminopropyl)carbodiimide hydrochloride (0.2 g) were introduced to AP-MSN (400 mg) in DMSO (20 mL) to yield the boronic acid-functionalized (0.5 mmol g^{-1}) MSN material (BA-MSN) (Figure 1b). The presence of both aminopropyl and phenylboronic acid groups stabilizes the formation of borates with 1,2- or 1,3-diols (Figure 1a). A fluorescein isothiocyanate (FITC)-labeled G-Ins (FITC-G-Ins) was prepared according to a literature procedure.⁸ The bioactivity of G-Ins was demonstrated to be similar to that of unmodified insulin.⁸ The mesopores of BA-MSN (100 mg) were loaded with cAMP (1 mM) in PBS buffer (10 mL, pH 7.4) and then capped with FITC-G-Ins (200 mg) through reversible covalent bonding between phenylboronic acid and the vicinal diols of FITC-G-Ins, giving rise to the desired FITC-G-Ins-MSN material (Figure 1c). The loadings of cAMP and FITC-G-Ins were determined to be 27 and $64 \mu\text{mol/g}$ by HPLC¹⁵ and fluorescence emission spectroscopy, respectively. As detailed in the SI, the structures and surface properties of BA-MSN and FITC-G-Ins-MSN

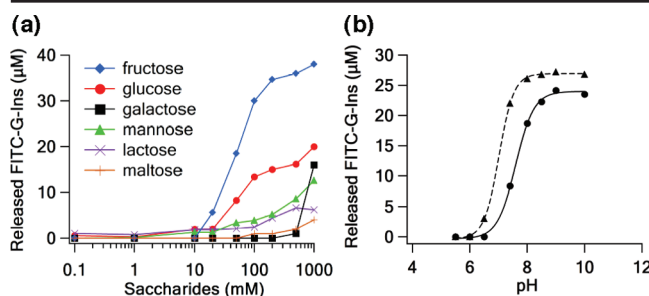


Figure 2. (a) Dependence of FITC-G-Ins release from FITC-G-Ins-MSN (2 mg mL^{-1} in PBS, pH 7.4) on the concentration of saccharide triggers. (b) pH titration of insulin release from FITC-G-Ins-MSN (2 mg mL^{-1} in PBS) triggered by 50 mM glucose (solid line) and 50 mM fructose (dashed line).

were characterized by powder X-ray diffraction (XRD), N_2 surface analysis, ζ potential measurements, and transmission electron microscopy.

As demonstrated in the literature,¹⁶ phenylboronic acid forms much more stable cyclic esters with the adjacent diols of saccharides than with acyclic diols. This means that the linkage between FITC-G-Ins and BA-MSN could be cleaved by introducing various saccharides. Therefore, it was expected that the release of FITC-G-Ins would be sensitive to the chemical structures and concentrations of different carbohydrate triggers in forming stable cyclic boronic esters with BA-MSN. Among different saccharide triggers, the release of FITC-G-Ins indeed showed a strong preference for fructose, followed by glucose, as shown in Figure 2a. The observed high selectivity for fructose is consistent with other reported monoboronic acid-based sensors for saccharide recognition.¹⁷ It is known that saccharides can interconvert between their pyranose and furanose isomeric forms, and phenylboronic acid has a strong preference for binding with the hydroxyls of saccharides in their furanose forms. The high selectivity toward fructose could be explained by its high percentage of furanose form in water (25% for fructose vs 0.14% for glucose).¹⁸

For monoboronic acids in water with 1:1 saccharide/boronic acid complexation, high selectivity for fructose and low selectivity for glucose were observed, and the difference was attributed to the relative percentage of the furanose forms of these carbohydrates.¹⁸ Interestingly, our system was highly responsive toward fructose and glucose in comparison with other saccharides (Figure 2a). This could be attributed to the heterogeneous spacing of boronic acid groups, which leads to the coexistence of 1:1 and 1:2 complexation, where the 1:2 complexation is widely used in the design of diboronic acid systems for selective glucose sensing.¹⁹ In contrast, disaccharides (lactose and maltose) were not able to adopt a furanose form and hence could not serve as effective triggers for pore uncapping. While a stronger preference for fructose than for glucose was observed, the FITC-G-Ins-MSN system is still suitable for glucose-responsive insulin release because of the much lower level of blood fructose ($\leq 0.1 \text{ mM}$) than of glucose ($\geq 10 \text{ mM}$) in diabetic patients.

The release of FITC-G-Ins triggered by any of the saccharides was found to be complete within 30 min, which is within the time frame of normal insulin secretion. The complexation of fructose and glucose with phenylboronic acid and the corresponding release of FITC-G-Ins exhibited a strong pH dependence. As shown in Figure 2b, the release of FITC-G-Ins triggered by 50 mM fructose reached 85% of maximum release at pH 7.4. In contrast, significant release of FITC-G-Ins was observed only at pH values above 8 in the case of glucose. This is likely due to the fact that the formation of tetrahedral borate intermediate requires a pH higher than the

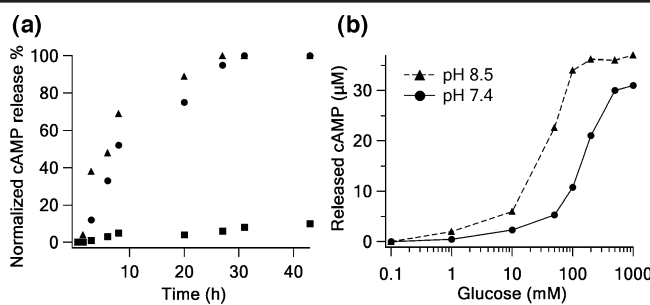


Figure 3. Controlled release of cAMP from FITC-G-Ins-MSN (2 mg mL^{-1} in PBS) (a) triggered by 50 mM glucose at pH 7.4 (●) and 8.5 (▲), with control data at pH 7.4 in the absence of glucose (■), and (b) triggered by different concentrations of glucose at pH 7.4 (solid line) and 8.5 (dashed line) measured 48 h after glucose treatment.

K_a of boronic acid. The observed pH dependence in our material, which is indicative of the controlled release mechanism, is consistent with those of other literature-reported insulin delivery systems.²⁰

To further examine the applicability of this system, FITC-G-Ins released by a stepwise treatment of glucose at two diabetic levels (50 and 100 mM) was monitored (Figure S6 in the SI). A typical decrease in insulin release after the second cycle was observed. However, this problem of decreasing insulin level could be overcome by delivering the cell-membrane-impermeable cAMP into the cytosol to stimulate insulin secretion from pancreas beta cells. This double-release system sets up a new model for self-regulated insulin-releasing devices.

The glucose-triggered release of cAMP by FITC-G-Ins uncapping was determined by HPLC¹⁵ at pH 7.4 and 8.5, as shown in Figure 3. In PBS (pH 7.4), the cAMP-loaded FITC-G-Ins-MSN exhibited less than 10% leaching in the absence of glucose trigger, suggesting a good capping efficiency of FITC-G-Ins. The rate of cAMP release triggered by 50 mM glucose at pH 7.4 and 8.5 showed similar diffusion-controlled kinetic profiles. Specifically, ~80% of total release was obtained within 20 h. Furthermore, 55 and 67% of the total loaded cAMP ($27 \mu\text{mol g}^{-1}$) were released after 30 h at pH 7.4 and 8.5, respectively (Figure 3a). As shown in Figure 3b, the release of cAMP strongly depends on the concentration of glucose. A significant cAMP release at pH 7.4 was observed when the concentration of glucose trigger was above 100 mM, whereas 50 mM glucose triggered almost 60% of maximum release at pH 8.5. This pH dependence of cAMP release is consistent with that of FITC-G-Ins release from MSN.

To correlate these *in vitro* results with the physiological concentrations for potential *in vivo* applications, the therapeutic dosage of this material was estimated. Between meals, the insulin level typically rises from a fasting level of 20–30 pM to a 30 min maximum of 250–300 pM, depending upon the amount and quality of carbohydrates consumed, while the diabetic insulin level remains at 20–30 pM or below. It has been reported in the literature that at least 250–300 pM of insulin is needed to decrease the diabetic blood glucose concentration to the normal level.²¹ Our results indicate that 20 mM glucose indeed induced the release of 2 μM G-Ins from our material at a concentration of 2 mg mL^{-1} (Figure 2a). Delivery of 250–300 pM of G-Ins would require only 0.25–0.3 $\mu\text{g mL}^{-1}$ MSN material, which is 4 orders of magnitude lower in concentration than what we have demonstrated above. As reported previously, the MSN dosage has a minimal effect on viability and proliferation of mammalian cells at concentrations below $100 \mu\text{g mL}^{-1}$ after 6 days.²² Also, the maximum concentration of cAMP released from 2 mg mL^{-1} G-Ins-MSN was $30 \mu\text{g mL}^{-1}$ (Figure 3b). On the basis of these results, we envision that the application of 0.25–0.30 $\mu\text{g mL}^{-1}$ G-Ins-MSN *in vivo* could sufficiently deliver

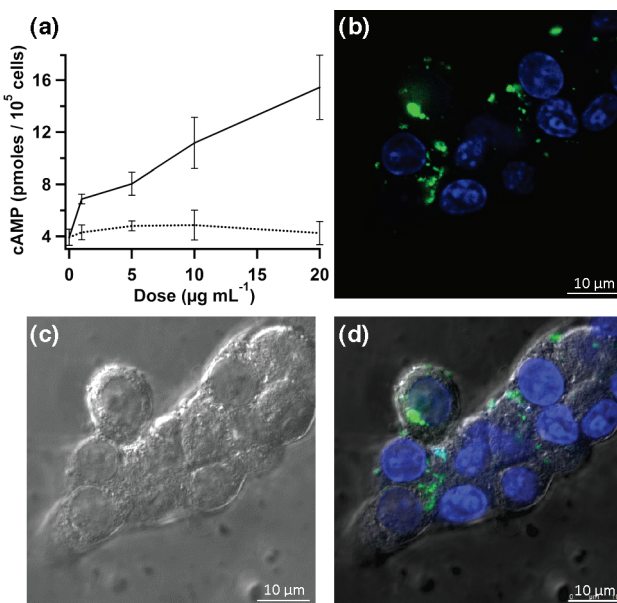


Figure 4. (a) Intracellular cAMP concentration of rat pancreatic RIN-5F cells treated with the cAMP-loaded BA-MSN (solid line) and free-solution cAMP (dashed line), measured after 6 h of introduction. (b) Fluorescence confocal micrograph of RIN-5F cells incubated with $20 \mu\text{g mL}^{-1}$ Fluoro-cAMP-loaded BA-MSN (green) for 6 h. Cell nuclei were stained with DAPI (blue). (c) Corresponding differential interference contrast (DIC) micrographs. (d) Fluorescence confocal and DIC merged image. Enlarged individual and merged images are shown in Figure S9 in the SI.

both G-Ins and cAMP for blood glucose regulation and insulin secretion, respectively, and would not produce any acute toxic effects.

To examine the cytotoxicity of the cAMP-loaded G-Ins-MSN material, cell viability and proliferation profiles of four different cell lines [rat pancreatic islet tumor (RIN-5F), mouse liver, skin fibroblast, and human cervical cancer (HeLa) cells] were evaluated by Guava ViaCount cytometry assay after 24 h inoculation with the material. Good cell viability (>90%) and proliferation (>80%) were observed for all cell lines containing 5 or $20 \mu\text{g mL}^{-1}$ G-Ins-MSN. These results further indicate that this MSN-based double delivery system is biocompatible.

The cellular uptake properties of the cAMP-loaded BA-MSN with and without G-Ins capping were investigated with RIN-5F cells. As detailed in the SI, BA-MSN labeled with FITC (FITC-BA-MSN) for this study was prepared prior to cAMP loading and G-Ins capping. The endocytosis efficiency was quantified by flow cytometry after 1 h of incubation with each material at $10 \mu\text{g mL}^{-1}$ (Figure S8). Interestingly, the cAMP-loaded FITC-BA-MSN without G-Ins capping showed a 2-fold higher endocytosis efficiency than that of the G-Ins-capped material. The result could be attributed to the difference in their surface charge properties: the ζ potentials were -28.3 mV for the uncapped material and -44.5 mV for the G-Ins-capped version.¹³ This difference between the endocytosis efficiencies of the capped and uncapped materials implies that G-Ins-MSN could circulate in the regulatory system before the glucose-induced G-Ins release, and the enhanced cellular uptake of cAMP-loaded BA-MSN after the pore uncapping would allow efficient intracellular cAMP delivery.

To quantify the degree of intracellular release of cAMP from our system, the cAMP-loaded BA-MSN was allowed to be internalized by RIN-5F cells. After 6 h of incubation, the total cellular concentration of cAMP was measured using a Millipore cAMP HTS immunoassay (see the SI). The result was compared

with that of RIN-5F cells introduced to free-solution cAMP. As shown in Figure 4a, the total cellular concentration of cAMP indeed increased proportional to the dosage of cAMP-loaded BA-MSN. In contrast, no significant elevation of the cellular concentration of cAMP was observed in the case of free-solution cAMP, even at the high dosage of $20 \mu\text{g mL}^{-1}$, which is consistent with the poor cell-membrane permeability of free-solution cAMP.

To visualize intracellular delivery of cAMP, a membrane impermeable, fluorescence-labeled cAMP (8-Fluo-cAMP)²³ was loaded into the BA-MSN. Fluo-cAMP-loaded BA-MSN ($20 \mu\text{g mL}^{-1}$) was incubated with RIN-5F cells for 6 h. The fluorescence confocal micrographs (Figure 4b–d) clearly showed that Fluo-cAMP-loaded BA-MSN was indeed internalized by live RIN-5F cells. Green fluorescence was observed for both Fluo-cAMP-loaded BA-MSN particles and the free Fluo-cAMP molecules released from the MSN intracellularly.

In conclusion, we have successfully demonstrated that phenylboronic acid-functionalized MSN can serve as an efficient codeelivery system for saccharide-responsive controlled release of insulin and cAMP. The good biocompatibility, cellular uptake properties, and efficient intracellular release of cAMP set up the basis for future *in vivo* controlled-release biomedical applications.

Acknowledgment. This research was supported by the U.S. National Science Foundation (CHE-0809521).

Supporting Information Available: Synthesis and characterization of AP-MSN, BA-MSN, and FITC-G-Ins-MSN; cell viability and proliferation assays; and flow cytometry, intracellular cAMP quantification, and confocal fluorescence microscopy studies. This material is available free of charge via the Internet at <http://pubs.acs.org>.

References

- For a review, see: Slowing, I. I.; Vivero-Escoto, J. L.; Wu, C.-W.; Lin, V. S. Y. *Adv. Drug Delivery Rev.* **2008**, *60*, 1278.
- For a review, see: Descalzo, A. B.; Martinez-Manez, R.; Sancenon, F.; Hoffmann, K.; Rurack, K. *Angew. Chem., Int. Ed.* **2006**, *45*, 5924.
- For a review, see: Angelos, S.; Liang, M.; Choi, E.; Zink, J. I. *Chem. Eng. J. (Amsterdam, Neth.)* **2008**, *137*, 4.
- Lee, C.-H.; Cheng, S.-H.; Wang, Y.-J.; Chen, Y.-C.; Chen, N.-T.; Souris, J.; Chen, C.-T.; Mou, C.-Y.; Yang, C.-S.; Lo, L.-W. *Adv. Funct. Mater.* **2009**, *19*, 215.
- Slowing, I. I.; Wu, C.-W.; Vivero-Escoto, J. L.; Lin, V. S. Y. *Small* **2009**, *5*, 57.
- Taylor, K. M. L.; Kim, J. S.; Rieter, W. J.; An, H.; Lin, W.; Lin, W. *J. Am. Chem. Soc.* **2008**, *130*, 2154.
- Wu, S.-H.; Lin, Y.-S.; Hung, Y.; Chou, Y.-H.; Hsu, Y.-H.; Chang, C.; Mou, C.-Y. *ChemBioChem* **2008**, *9*, 53.
- Shiino, D.; Kataoka, K.; Koyama, Y.; Yokoyama, M.; Okano, T.; Sakurai, Y. *J. Intell. Mater. Syst. Struct.* **1994**, *5*, 311.
- Shiino, D.; Murata, Y.; Kubo, A.; Kim, Y. J.; Kataoka, K.; Koyama, Y.; Kikuchi, A.; Yokoyama, M.; Sakurai, Y.; Okano, T. *J. Controlled Release* **1995**, *37*, 269.
- Charles, M. A.; Fanska, R.; Schmid, F. G.; Forsham, P. H.; Grodsky, G. M. *Science* **1973**, *179*, 569.
- Dyachok, O.; Ideval-Hagren, O.; Saagertorp, J.; Tian, G.; Wuttke, A.; Arriemeirou, C.; Akusjaervi, G.; Gylfe, E.; Tengholm, A. *Cell Metab.* **2008**, *8*, 26.
- Schultz, C.; Vajanaphanich, M.; Genieser, H.-G.; Jastorff, B.; Barrett, K. E.; Tsien, R. Y. *Mol. Pharmacol.* **1994**, *46*, 702.
- Slowing, I.; Trewyn, B. G.; Lin, V. S. Y. *J. Am. Chem. Soc.* **2006**, *128*, 14792.
- Awasthi, V. D.; Garcia, D.; Goins, B. A.; Phillips, W. T. *Int. J. Pharm.* **2003**, *253*, 121.
- Hoewer, H.; Zoch, E. *Fresenius' Z. Anal. Chem.* **1987**, *327*, 555.
- Springsteen, G.; Wang, B. *Tetrahedron* **2002**, *58*, 5291.
- Phillips, M. D.; James, T. D. *J. Fluoresc.* **2004**, *14*, 549.
- Lorand, J. P.; Edwards, J. O. *J. Org. Chem.* **1959**, *24*, 769.
- Fang, H.; Kaur, G.; Wang, B. *J. Fluoresc.* **2004**, *14*, 481.
- Matsumoto, A.; Ikeda, S.; Harada, A.; Kataoka, K. *Biomacromolecules* **2003**, *4*, 1410.
- Suckale, J.; Solimena, M. *Front. Biosci.* **2008**, *13*, 7156.
- Radu, D. R.; Lai, C.-Y.; Jeftinija, K.; Rowe, E. W.; Jeftinija, S.; Lin, V. S. Y. *J. Am. Chem. Soc.* **2004**, *126*, 13216.
- Moll, D.; Prinz, A.; Brendel, C. M.; Berrera, M.; Guske, K.; Zaccole, M.; Genieser, H.-G.; Herberg, F. W. *BMC Biochem.* **2008**, *9*, 18.

JA901831U

Supporting Information

Mesoporous Silica Nanoparticle-based Double Drug Delivery System for Glucose Responsive Controlled Release of Insulin and Cyclic AMP

Yannan Zhao, Brian G. Trewyn, Igor I. Slowing, and Victor S.-Y. Lin*

Department of Chemistry, U.S. Department of Energy Ames Laboratory, Iowa State University, Ames, Iowa 50011-3111, U.S.A.

1. Experimental

1.1 Synthesis of AP-MSN

N-Cetyltrimethylammonium bromide (CTAB, 1.00 g, 2.74 mmol) was dissolved in 480 mL of nanopure water. Sodium hydroxide aqueous solution (2.00 M, 3.50 mL) was introduced to the CTAB solution and the temperature of the mixture was adjusted to 353 K. Tetraethoxysilane (TEOS, 5.00 mL, 22.4 mmol) was added dropwise to the surfactant solution under vigorous stirring. The mixture was allowed to react for 2 h to give rise to a white precipitate. This solid crude product was filtered, washed with nanopure water and methanol, and dried under high vacuum to yield the as-synthesized MSN. To remove the surfactant template (CTAB), 1.50 g of the as-synthesized MSN was refluxed for 6 h in a methanolic solution of 1.50 mL HCl (37.2%) in 150 mL methanol. The resulting material was filtered and extensively washed with nanopure water and methanol. The surfactant-free MSN material was placed under high vacuum with heating at 333 K to remove the remaining solvent from the mesopores. MSN (1.00 g) was refluxed for 20 h in 80.0 mL of anhydrous toluene with 1.00 mL (5.67 mmol) of 3-aminopropyltrimethoxysilane to yield the 3-aminopropyl-functionalized MSN (AP-MSN) material. The surface amine groups were quantified at 1.6 mmol/g by ninhydrin test.¹

1.2 Synthesis of BA-MSN

The purified AP-MSN (400 mg) was dispersed in 20 mL dimethyl sulfoxide (DMSO). 0.15 g (0.90 mmol) 4-carboxyphenylboronic acid (CBA) was reacted with 0.10 g (0.87 mmol) N-hydroxysuccinimide (NHS) and 0.20 g (1.04 mmol) 1-ethyl-3-(3-dimethylaminopropyl) carbodiimide hydrochloride (EDC) in 5.0 mL DMSO, stirring at room temperature for 15 min before adding to the AP-MSN suspension. The mixture was stirred at room temperature for another 24 h, followed by filtration and washing with DMSO, water and methanol. The remaining surface amine groups were quantified at 1.1 mmol/g by ninhydrin test,¹ and surface boronic acid groups were calculated to be around 0.5 mmol/g by subtracting the amount of remaining surface amine groups from that on AP-MSN surface.

1.3 Synthesis of FITC-G-Ins

Gluconic acid modified insulin (G-Ins) was prepared according to the reported procedure,² and was further labeled with FITC for *in vitro* controlled release study. G-Ins (200 mg) was dissolved in 50 mL sodium carbonate buffer (0.1 M, pH 9), and 2.5 mL FITC in DMSO (1 mg/mL) was added in 5 μ L aliquots while gently stirring the G-ins solution in dark. The reaction was stirred for another 2 h at room temperature before adding NH₄Cl (2.5 mL, 1 M) to quench excess FITC. After stirring for another 1 h, the solution was dialyzed in phosphate-buffered saline (PBS) (Spectra/Por 3, MWCO = 3500, Spectrum) and freeze dried to yield FITC labeled G-Ins (FITC-G-Ins). The ratio of FITC to G-ins was estimated at 1.3 by measuring the absorbance at 495 nm and 280 nm.

1.4 Synthesis of cAMP loaded FITC-G-Ins-MSN

The purified BA-MSN (100.0 mg) was stirred in a solution of cAMP (1 mM) in PBS solution (10 mL, 154 mM, pH 7.4) for 24 h in dark. Then, FITC-G-Ins (200 mg) was added to the suspension. The mixture was stirred in dark for another 24 h, following by filtration and washing extensively with PBS to remove physisorbed, uncapped cAMP and uncoated FITC-G-Ins from the exterior surface of the material. The resulting precipitate was isolated and dried under high vacuum. The loading of cAMP (27 μ mol/g) and FITC-G-Ins (64 μ mol/g) was calculated by subtracting the amount of cAMP/FITC-G-insulin remaining in the phosphate buffer and combined washings from the amount of cAMP/insulin initially added to the reaction.

1.5 Saccharides triggered G-Ins and cAMP release study

Cyclic AMP loaded FITC-G-Ins-MSN (6.00 mg) was dispersed in 3.00 mL of PBS with different concentrations of saccharides triggers. Aliquots (1.5 mL) were taken after 2 days stirring in dark at room temperature, followed by centrifuge (14000 rpm, 20 min). The release of FITC-G-Ins was determined by fluorescence emission spectroscopy (exc. at 488 nm, em. at 515 nm). The release of cAMP was monitored by HPLC (Hitachi LC/3DQMS with a reverse phase C18 column (Vydac), 0.4 cm x 25 nm), according to the literature reported method.³ For the release kinetics study, cAMP loaded FITC-G-Ins-MSN (30.00 mg) was dispersed in 15.00 mL of PBS with 50 mM glucose. Aliquots (1.2 mL) were taken periodically from the suspension, followed by centrifuge (14000 rpm, 20 min), and the release kinetics of FITC-G-Ins and cAMP were monitored by fluorescence emission spectroscopy and HPLC, respectively.

1.6 G-Ins release study by stepwise glucose treatment

Cyclic AMP loaded FITC-G-Ins-MSN (20.00 mg) was dispersed in 10.00 mL of PBS and treated with 50 mM/ 100 mM glucose every 50 min. The release of FITC-G-Ins was monitored after 10 and 30 min glucose treatment, immediately followed by washing with 10.00 mL fresh PBS without glucose. The concentration of FITC-G-Ins in the washing PBS was recorded as the data point 40 min after treatment. The treatment was repeated until the release of FITC-G-Ins was stable without any increase (Figure S6).

2. Characterization

2.1 Powder X-Ray Diffraction

X-ray diffraction patterns of the MSN materials were obtained in a Scintag XDS-2000 powder diffractometer using Cu K α irradiation.

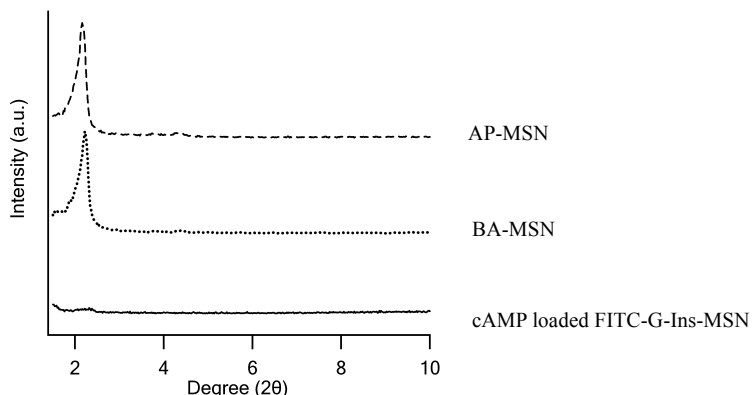


Figure S1. Powder X-Ray Diffraction patterns of AP-MSN, BA-MSN, and cAMP loaded FITC-G-Ins-MSN. Both AP-MSN and BA-MSN exhibit the typical diffraction patterns of MCM-41 type mesoporous silica with hexagonal symmetry. The changes in the cAMP loaded FITC-G-Ins-MSN diffraction pattern might be caused by pore filling and insulin coating effects.

Table S1. Powder X-Ray diffraction patterns

Material	d_{100} (Å)	a_0 (Å)	$d_{\text{pore wall}}$ (Å)
AP-MSN	40.9	47.2	6.3
BA-MSN	39.7	45.8	6.1

The d_{100} numbers represent the d-spacing corresponding to the main (100) XRD peak. The unit-cell size (a_0) is calculated from the d_{100} data using the formula $a_0 = 2 d_{100}/3^{1/2}$. The pore wall thickness $d_{\text{pore wall}} = a_0 - W_{\text{BJH}}$.

2.2 Nitrogen adsorption/desorption isotherms

Surface analysis of the MSN materials was performed by nitrogen sorption isotherms in a Micromeritics Tristar 3000 sorptometer. The surface areas were calculated by the Brunauer–Emmett–Teller (BET).

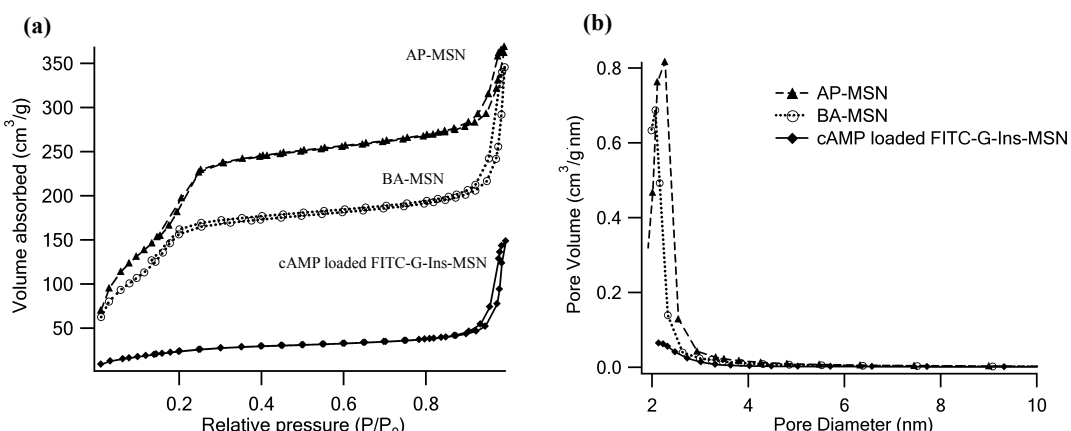


Figure S2. BET nitrogen adsorption/desorption isotherms (a) and BJH pore size distributions (b) of AP-MSN, BA-MSN and cAMP loaded FITC-G-Ins-MSN.

Table S2. BET and BJH parameters

Material	BET surface area S_{BET} (m^2/g)	BET Pore Volume V_p (cm^3/g)	BJH Pore diameter W_{BJH} (\AA)
AP-MSN	708.2	0.652	23
BA-MSN	634.6	0.520	21
cAMP loaded FITC-G-Ins-MSN	93.8		

2.3 Transmission Electron Micrographs (TEM) of BA-MSN and FITC-G-Ins-MSN

The TEM examination was completed on a Tecnai G2 F20 electron microscope operated at 200 kV to examine at electron optical magnification of 64,000 to 550,000.

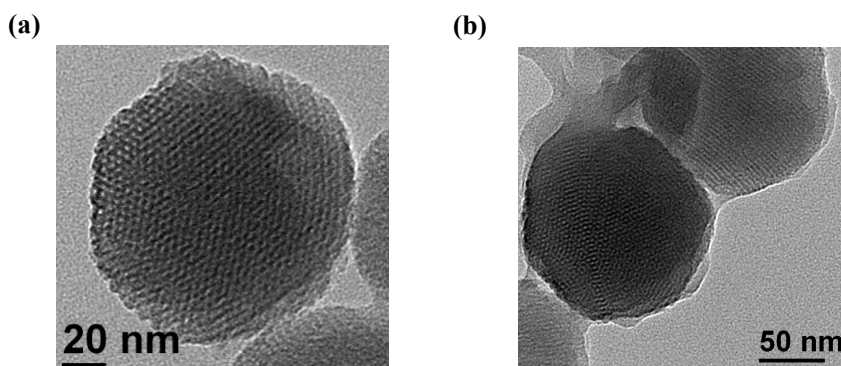


Figure S3. TEM micrographs of BA-MSN (a) and FITC-G-Ins-MSN (b).

2.4 Surface charge

The ζ -potential of the MSN materials was measured in a Malvern Nano HT Zetasizer. 200 $\mu\text{g/mL}$ suspensions of each of the materials in PBS (20 mM, pH 7.4) were prepared for this measurement.

Table S3. ζ -potential results

Material	ζ -potential (mV)
AP-MSN	+ 5.86
BA-MSN	- 14.6
cAMP loaded FITC-G-Ins-MSN	- 44.8

2.5 Alizarin Red S. (ARS) assay for boronic acid groups of BA-MSN

The stability and binding ability of boronic acid groups on BA-MSN surface was examined using the fluorescent reporter Alizatin Red S. (ARS), according to published literature procedures.^{4,5} The fluorescence intensities were measured with an excitation wavelength of 468 nm and an emission wavelength of 572 nm. A typical set of fluorescence spectra, which reflect the large changes in fluorescence intensity upon addition of BA-MSN to an ARS solution, is shown in figure S4.

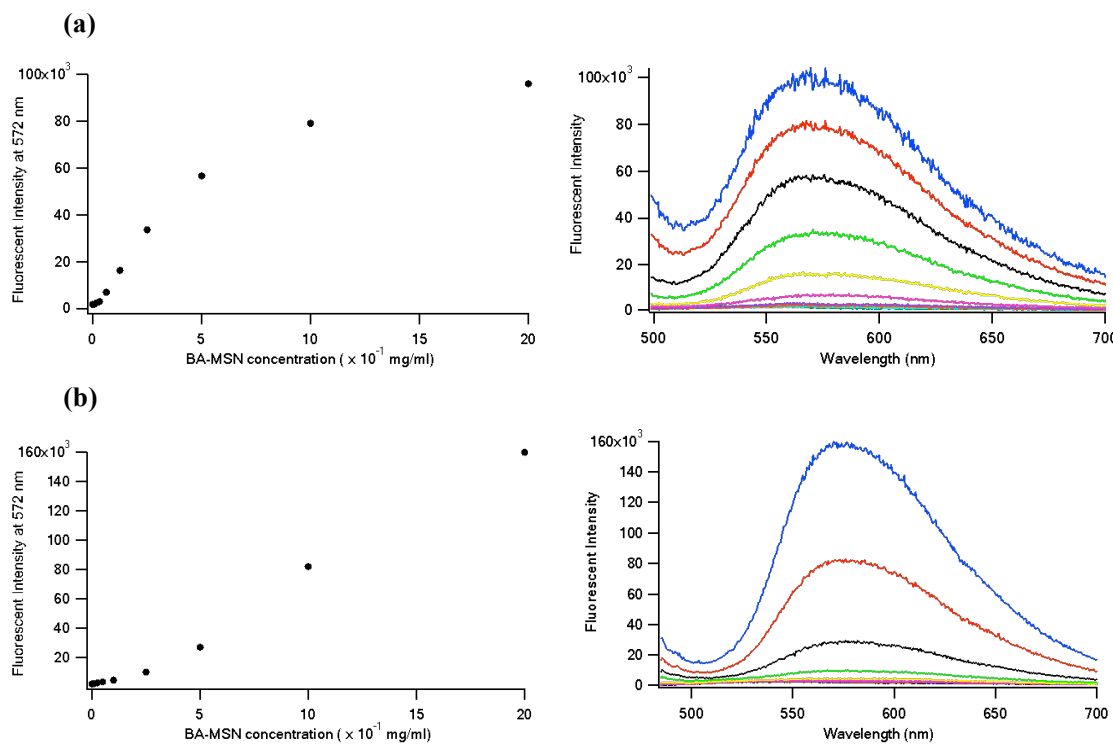


Figure S4. Fluorescent intensity increases (Exc. $\lambda = 468$ nm, Em. $\lambda = 572$ nm) with added BA-MSN (0 through 2.0 mg/mL) into a solution of ARS (a) 1.0×10^{-5} M (b) 1.0×10^{-4} M, in PBS (pH 7.4).

2.6 Competitive binding examination of BA-MSN with Alizarin Red S. and glucose

When glucose was added to the mixture of BA-MSN and ARS, fluorescence intensity decreases were observed. Titrating glucose into an aqueous solution of 1.0×10^{-4} M ARS and 0.4 mg/mL BA-MSN caused a significant drop in fluorescence intensity at glucose concentration over 50 mM, and a measurable change down to 10 mM.

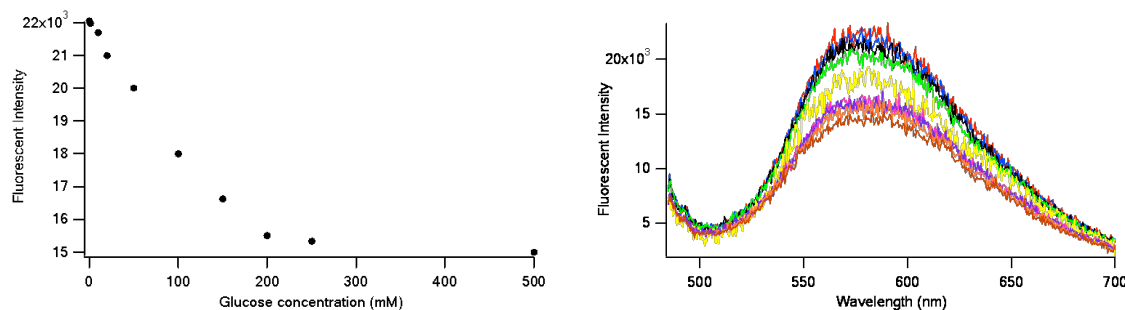


Figure S5. Titration of glucose into a solution of ARS (1.0×10^{-4} M) and BA-MSN (0.4 mg/mL). Fluorescence decreases (Exc. $\lambda = 468$ nm, Em. $\lambda = 572$ nm) with added glucose (0 through 0.5 M), in PBS (pH 7.4).

2.7 FITC-G-Ins release by stepwise glucose treatment

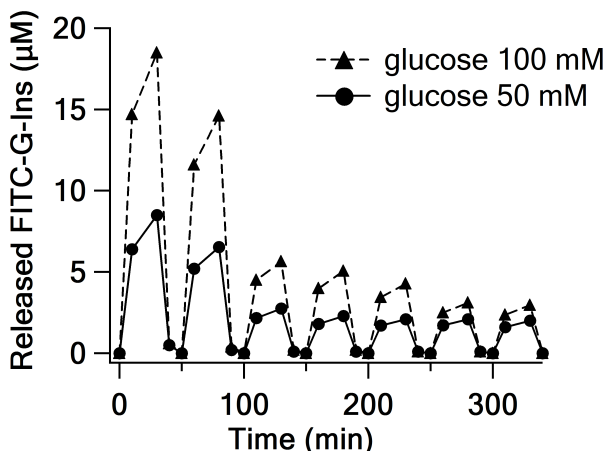


Figure S6. FITC-G-Ins release from FITC-G-Ins-MSN (2 mg mL⁻¹ in PBS, pH 7.4) by stepwise glucose treatment with 50 mM glucose (solid line) and 100 mM glucose (dashed line). Glucose was introduced every 50 min and removed by PBS washing 30 min post-treatment.

3. Biological studies

Reagents and materials for biological studies

Rat islet tumor (RIN-5F), mouse liver, skin fibroblast, HeLa cell line was obtained from American Tissue Culture Collection (ATCC). Formaldehyde solution (37%, w/w) was purchased from Fisher. 4,6-Diamidino-2-phenylindole dihydrochloride (DAPI) and trypan blue solution (0.4%, w/w) were purchased from Sigma-Aldrich. Trypsin (1×, 0.25%) in 0.1% EDTA-Na without calcium and magnesium was purchased from Fisher Scientific. 8-(2-[Fluoresceinyl]aminoethylthio)-adenosine-3',5'-cyclic monophosphate (8-Fluo-cAMP) was purchased from Axxora, LLC. Cyclic AMP HTS Immunoassay kit was purchased from Millipore.

Cell line maintenance

Rat islet tumor (RIN-5F) cells were maintained in T75 flasks using ATCC formulated RPMI-1640 medium supplemented with 10% (v/v) fetal bovine serum, 100 U/mL penicillin, and 100 µg/mL streptomycin. The medium was renewed every 3-4 days. Subculture was performed every 6-8 days at a ratio of 1:3-1:5.

Mouse liver, skin fibroblast and HeLa cells were maintained in T75 flasks using the base medium DMEM (Dulbecco's modified Eagle's medium) supplemented with 2 mM l-glutamine, 100 U/mL penicillin, 100 µg/mL streptomycin, and 1 mg/mL gentamycin. To make the complete growth medium, 10% (v/v) fetal bovine serum is added for liver and skin fibroblast cells culture, and 10% (v/v) equine serum is added for HeLa cells. Subculture was performed every 3-5 days for liver and skin fibroblast cell lines, and every 2-3 days for HeLa cells at a ratio of 1:3-1:5.

3.1 Cell viability and proliferation study

To eliminate any interference caused by FITC, G-Ins was used instead of FITC-G-Ins for capping upon cAMP loading, and G-Ins capped BA-MSN (G-Ins-MSN) was used for cytotoxicity

study described here.

Rat islet tumor (RIN-5F), liver, skin fibroblast and HeLa cells were seeded in 6-well plates at the concentration of 1×10^5 cells/mL and were incubated for 48 h in standard culture medium at 37 °C in 5% CO₂. After 48 h, the cells were inoculated with 5.0 µg/mL and 20.0 µg/mL of cAMP loaded G-Ins-MSN, and grown for an additional 24 h. As a control experiment, the cells were incubated with standard growth medium without cAMP loaded G-Ins-MSN for another 24 h. Finally, the cytotoxicity of this material with different cell lines was evaluated by Guava ViaCount cytometry assay (Guava Technologies, Inc.; Hayward, CA). Cell viability was calculated as a percentage of viable cells 24 h post-treatment with cAMP loaded G-Ins-MSN compared with untreated cells. Cell proliferation was calculated as a percentage of the total number of cells after G-Ins-MSN treatment out of the total number of untreated cells. Figure S7 shows the results of the cell counts 24 post-treatment. The viability was found to be between 90 and 100%, and the proliferation to be between 80 and 100%.

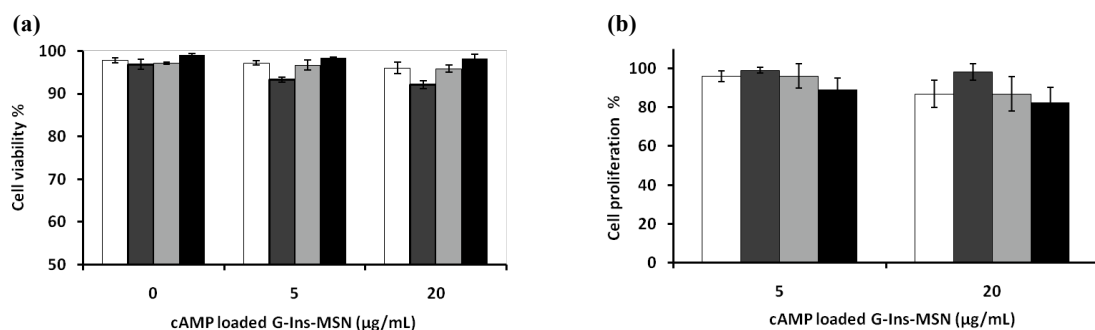


Figure S7. (a) Cell viability and **(b)** proliferation study of cAMP loaded G-Ins-MSN with rat pancreatic RIN-5F (white), mouse liver (dark grey), skin fibroblast (light grey) and HeLa (black) cells. The concentrations of the material used were 5 and 20 µg/mL.

3.2 Measuring the endocytosis efficiency with RIN-5F cells

BA-MSN was labeled for this endocytosis study by reacting 200 mg of BA-MSN with 7.8 mg (0.1 mmol) fluorescein isothiocyanate (FITC) in 20 mL methanol at room temperature for 2 h. The resulting product was filtered and washed with methanol extensively to remove physisorbed FITC. cAMP loaded FITC-BA-MSN was then prepared by incubating 10 mg of FITC-BA-MSN with 1 mM cAMP in 2 mL PBS solution (154 mM, pH 7.4) at room temperature in dark for 24 h with stirring, and cAMP loaded G-Ins-FITC-MSN was prepared by further capping with 20 mg of G-Ins in 2 mL of 1 mM cAMP PBS solution for another 24 h incubation, following by filtration and washing with PBS. The zeta potential was determined to be -28.3 mV for the “uncapped” cAMP loaded FITC-BA-MSN material and -44.5 mV for the “G-Ins-capped” cAMP loaded G-Ins-FITC-MSN.

The RIN-5F cells at a concentration of 1×10^5 cells/mL were grown in 6-well plates for 72 h at 37 °C in 5% CO₂. The cells were then treated with 10 µg/mL of cAMP loaded FITC-BA-MSN and cAMP loaded G-Ins-FITC-MSN suspended in serum-free media and were incubated for another 1 h at 37 °C in 5% CO₂. After 1 h, the cells were washed once with PBS and trypsinized. The cells were incubated in 830 mM trypan blue for 10 min to quench the fluorescence of any MSN nanoparticles adhered to the exterior of the cells. The cellular uptake was measured by flow cytometry.

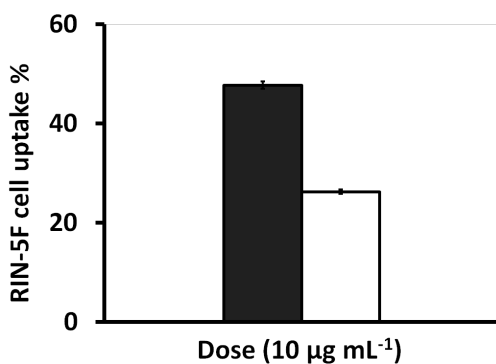


Figure S8. Rat pancreatic RIN-5F cellular uptake of $10 \mu\text{g/mL}$ of cAMP loaded FITC-BA-MSN (filled) and cAMP loaded G-Ins-FITC-MSN (open).

3.3 Fluorescence confocal microscopy measurements

To visually investigate the endocytosis and intracellular cAMP delivery by this material, fluorescence confocal microscopy measurement was employed. A membrane impermeable cAMP analogue 8-Fluo-cAMP was loaded to BA-MSN for the visualization of drug delivery, same procedure as described above for cAMP loading. Coverslips (22 mm^2) were cleaned with 1.0 M HCl , nanopure water ($3\times$), 50% ethanol, 70% ethanol, and 100% ethanol, and dried overnight at 60°C . Following cleaning, the coverslips were placed on the bottom of the wells of 6-well plates and covered with 3.0 mL of standard growth media. RIN-5F cells ($1.0 \times 10^5 \text{ cells/mL}$) were grown for 72 h on the coverslips. After 72 h , the cells were inoculated with $20.0 \mu\text{g/mL}$ of Fluo-cAMP loaded FITC-MSN, and grown for an additional 6 h . Afterwards, the growth media was removed, the cells were washed with PBS ($2\times$), and the cells were then reincubated with a PBS solution of 3.7% formaldehyde and 57.0 mM 4,6-Diamidino-2-phenylindole dihydrochloride (DAPI) for 30 min . These coverslips were removed from the PBS solution and fixed to glass slides with liquid adhesive.

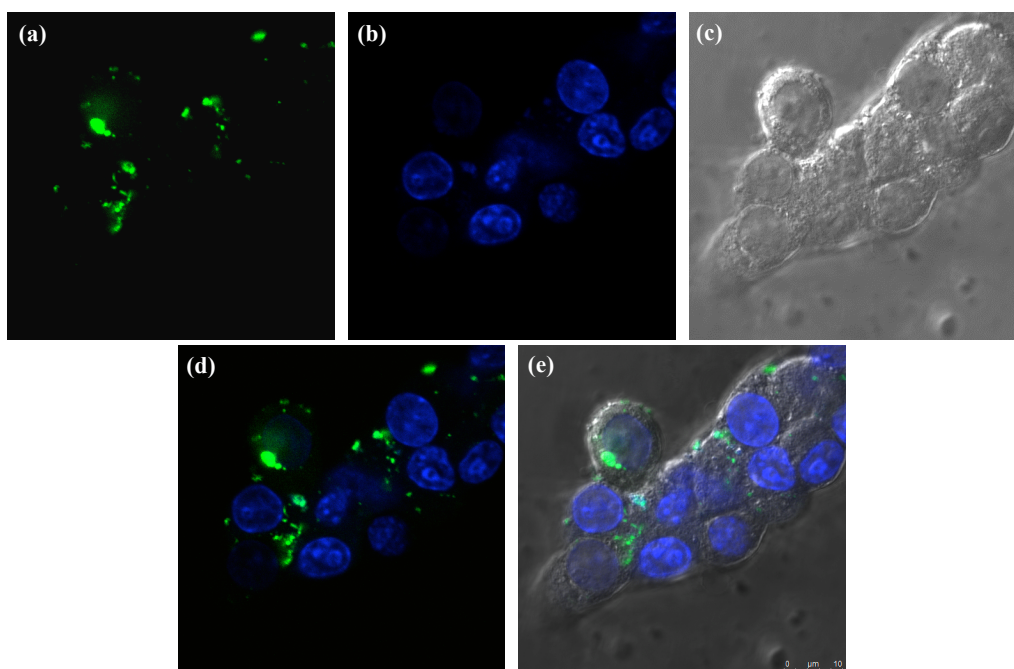


Figure S9. Fluorescence confocal micrographs of RIN-5F cells (a) internalized with $20 \mu\text{g mL}^{-1}$ suspension of Fluo-cAMP loaded BA-MSN (green) and (b) stained with 57.0 mM of DAPI (blue).

The corresponding Differential Interference Contrast (DIC) micrograph is displayed in image **(c)**. The image **(a)** and **(b)** merged micrograph and the image **(a)** **(b)** and **(c)** merged micrograph are shown in image **(d)** and **(e)**, respectively.

3.4 Quantification of intracellular cAMP delivery

The intracellular cAMP concentration was determined by a Millipore's cAMP High Throughput Screening (HTS) Immunoassay kit according to the manufacturer's directions. RIN-5F cells (1×10^5 cells/mL) were seeded in 48-well plates for 72 h at 37 °C in 5% CO₂. The cells were then treated with incremental amounts (0, 1, 5, 10, 20 µg/mL) of cAMP loaded BA-MSN suspended in serum-free media for 6 h at 37 °C in 5% CO₂. After 6 h, Adherent cells were washed five times with PBS to remove extracellular MSN particles and lysed for the intracellular cAMP assay or trypsinized for cell count by Guava ViaCount cytometry assay. The cellular cAMP levels were reported as pmoles/ 10^5 cells.

References:

- (1) Leane, M. M.; Nankervis, R.; Smith, A.; Illum, L. *Int. J. Pharm.* **2004**, *271*, 241-249.
- (2) Shino, D.; Kataoka, K.; Koyama, Y.; Yokoyama, M.; Okano, T.; Sakurai, Y. *J. Intell. Mater. Syst. Struct.* **1994**, *5*, 311-14.
- (3) Hoewer, H.; Zoch, E. *Fresenius' Z. Anal. Chem.* **1987**, *327*, 555-7.
- (4) Springsteen, G.; Wang, B. *Chem. Commun.* **2001**, 1608-1609.
- (5) Springsteen, G.; Wang, B. *Tetrahedron* **2002**, *58*, 5291-5300.